Publishing Excellence
Inspiring Progress
ARISTON PUBLICATIONS

Energy & Environment Advances

ISSN: xxxx-xxxx https://aristonpubs.com/energy-environment-advances https://doi.org/10.69626/eea.2024.0025

RESEARCH ARTICLE

Enhanced Electrical Conductivity and Photocatalytic Activity of Iron–Doped $CuAlO_2$ Nanoparticles for Sustainable Energy Applications

Azra Parveen *, Mohahmmad Zaid

ABSTRACT: This study investigates the impact of iron doping at the copper site in $CuAlO_2$ nanoparticles ($Cu_{0.9}Fe_{0.1}AlO_2$) on their electrical conductivity and photocatalytic activity, with a focus on energy harvesting applications. The nanoparticles were synthesized using a cost-effective sol-gel method and characterized by X-ray diffraction (XRD), Fourier Transform Infrared Spectroscopy (FTIR), and UV-visible spectroscopy. Structural analysis confirmed the successful incorporation of iron into the $CuAlO_2$ lattice without altering the delafossite crystal structure, while optical studies revealed an absorption edge suitable for visible light applications, with a band gap of approximately 2.8 eV. Electrical measurements demonstrated a significant enhancement in conductivity, attributed to additional charge carriers introduced by Fe doping. Photocatalytic activity was evaluated by degrading methylene blue dye under visible light irradiation, achieving 34% degradation within 140 minutes. Although the photocatalytic performance was moderate, it showcased potential for improvement through process optimization. The enhancement in electrical and photocatalytic properties was linked to improved charge carrier mobility, reduced recombination rates, and increased light absorption. This study highlights the dual functionality of Fe-doped $CuAlO_2$ nanoparticles, combining superior electrical conductivity with photocatalytic activity, making them promising materials for renewable energy and environmental applications. Further optimization of synthesis parameters and dopant concentration could unlock their full potential in solar energy harvesting, photocatalysis, and advanced optoelectronic devices.

Keywords: Fe-doped $CuAlO_2$, Electrical conductivity, Photocatalytic activity, Methylene blue degradation, Energy harvesting

Received: 20 January 2024; Revised: 19 February 2024; Accepted: 22 February 2024; Published Online: 01 March 2024

1. INTRODUCTION

The rapid depletion of fossil fuel reserves and growing environmental concerns have emphasized the urgent need for sustainable and renewable energy sources [1]. Solar energy, as one of the most abundant and clean energy resources, has garnered significant attention in recent years [2]. Developing advanced materials capable of efficiently converting solar energy into chemical energy has become a cornerstone of modern energy research [3]. Among these materials, delafossite-type oxides, particularly copper aluminum oxide ($CuAlO_2$), have emerged as a promising candidate due to their exceptional electrical conductivity, optical transparency, and catalytic efficiency [4-6]. These unique properties position $CuAlO_2$ as an ideal material for applications in photovoltaic cells, optoelectronic devices, sensors, and photocatalysis [7-9].

$CuAlO_2$ belongs to the family of delafossite-type oxides characterized by a layered crystal structure comprising alternating layers of Cu-O and Al-O bonds [10]. This structure contributes to its p-type semiconducting behavior, with a direct band gap that facilitates efficient charge transport and light absorption. Moreover, the material's inherent transparency in the visible region and excellent

Department of Applied Physics, Zakir Husain College of Engineering and Technology, Aligarh Muslim University, Aligarh, Uttar Pradesh-202002, India

* Author to whom correspondence should be addressed: azrap2001@gmail.com (Azra Parveen)

thermal stability make it highly versatile for diverse applications. However, the intrinsic properties of $CuAlO_2$ can be further tailored through doping, enabling researchers to fine-tune its electrical, optical, and catalytic characteristics for specific applications.

Doping with transition metals, particularly iron (Fe), has proven to be an effective strategy for enhancing the functional properties of $CuAlO_2$ nanoparticles [11-13]. Iron doping introduces additional energy levels within the band gap, thereby facilitating charge carrier generation and separation. This modification not only improves electrical conductivity but also enhances the photocatalytic activity of $CuAlO_2$ by increasing its light absorption capacity and promoting the generation of reactive oxygen species. These reactive species play a crucial role in applications such as organic pollutant degradation and water-splitting reactions, which are vital for environmental remediation and hydrogen production [14].

The photocatalytic efficiency of Fe-doped $CuAlO_2$ is further attributed to its ability to extend light absorption into the visible spectrum [15-17]. While pristine $CuAlO_2$ predominantly absorbs ultraviolet light, iron doping shifts the absorption edge, enabling the material to harness a broader range of the solar spectrum. This extended absorption, coupled with efficient charge carrier dynamics, significantly enhances the photocatalytic performance of Fe-doped $CuAlO_2$, making it a strong contender for applications in energy harvesting and environmental cleanup technologies [18].

Beyond photocatalysis, Fe-doped $CuAlO_2$ nanoparticles exhibit immense potential in energy harvesting systems, such as dye-sensitized solar cells (DSSCs) and photoelectrochemical (PEC) cells. In these systems, the efficient generation and transport of charge carriers are critical for maximizing energy conversion efficiency [19, 20]. Iron doping not only improves the electrical conductivity of $CuAlO_2$ but also enhances its absorption spectrum, thereby increasing the overall efficiency of solar energy conversion. The synergistic effect of improved charge transport and broadened light absorption makes Fe-doped $CuAlO_2$ a valuable material for next-generation energy technologies [21, 22].

Moreover, the structural properties of Fe-doped $CuAlO_2$ play a pivotal role in its performance. The sol-gel synthesis method, employed in this study, offers precise control over the material's morphology, particle size, and dopant distribution. This method ensures the uniform incorporation of Fe ions into the $CuAlO_2$ matrix, resulting in consistent and reproducible properties. Understanding the correlation between Fe concentration and the resulting structural, optical, and electrical properties is essential for optimizing the material's performance in various applications. The environmental benefits of Fe-doped $CuAlO_2$ are equally noteworthy. The material's enhanced photocatalytic activity enables the efficient degradation of organic pollutants, such as dyes and pesticides, in wastewater. Additionally, its potential for hydrogen production through water splitting addresses the growing demand for clean and renewable energy sources. These applications align with global efforts to mitigate environmental pollution and transition toward a sustainable energy future.

In this study, we focus on the synthesis and characterization of Fe-doped $CuAlO_2$ nanoparticles using the sol-gel method. The research aims to elucidate the impact of varying Fe concentrations on the structural, optical, and electrical properties of $CuAlO_2$. By investigating the material's electrical conductivity and photocatalytic activity, we seek to uncover the underlying mechanisms that drive its enhanced performance. This comprehensive analysis provides valuable insights into the design and optimization of $CuAlO_2$-based materials for a wide range of applications, including energy harvesting and environmental remediation. The findings of this study contribute to the broader field of materials science and renewable energy research. By demonstrating the potential of Fe-doped $CuAlO_2$ as a multifunctional material, we aim to pave the way for its integration into practical devices and systems. The knowledge gained from this research not only advances our understanding of delafossite-type oxides but also underscores the importance of material innovation in addressing global energy and environmental challenges.

2. EXPERIMENTAL DETAILS

2.1. Synthesis of the material

To synthesize Fe-doped $CuAlO_2$ nanoparticles (NPs), a simple and cost-effective sol-gel auto-combustion method was employed. The precursor materials used were of high analytical grade, including Copper (II) nitrate ($Cu(NO_3)_2 \cdot 6H_2O$, Sigma-Aldrich, 99.99%), Ferric (II) nitrate ($Fe(NO_3)_3 \cdot 9H_2O$, Sigma-Aldrich, 99.99%), and Aluminum (III) nitrate ($Al(NO_3)_3 \cdot 9H_2O$, Sigma-Aldrich, 99.99%). Citric acid was used as a chelating agent, while ammonia was used to adjust the pH. Deionized water served as the solvent to prepare the solutions.

The synthesis of Fe-doped $CuAlO_2$ nanoparticles ($Cu_{0.9}Fe_{0.1}AlO_2$) began by dissolving stoichiometric amounts of copper nitrate, ferric nitrate, and aluminum nitrate in deionized water to form a clear solution. The molar ratios of the components were carefully calculated to maintain the desired doping concentration of Fe in the $CuAlO_2$ lattice. Citric acid was added to the solution in a 1:1 molar ratio with the metal nitrates to act as a chelating agent. Ammonia was gradually added dropwise to adjust the pH of the solution to around 7, ensuring uniform mixing and gel formation. The resulting solution was continuously stirred and heated at 80°C for six hours. During this process, the solution transitioned into a viscous sol-gel state. The gel was then subjected to further heating at 100–120°C to initiate auto-combustion, producing a loose, black powder. The auto-combustion reaction released gaseous byproducts, leaving behind a precursor powder.

The precursor powder was collected and finely ground

using a mortar and pestle for one hour to ensure uniform particle size distribution. The powder was then calcined at 750°C for six hours in a muffle furnace. This calcination step was essential for achieving a pure-phase, fully crystalline sample. The high-temperature environment facilitated the formation of the delafossite structure and ensured the incorporation of Fe ions into the $CuAlO_2$ lattice.

2.2. Characterization

The phase purity and crystalline structure of the synthesized Fe-doped $CuAlO_2$ nanoparticles were analyzed using a Shimadzu LabX XRD-6100 diffractometer equipped with Cu-Kα radiation (λ = 1.5406 Å) at room temperature. The XRD data were collected over a 2θ range of 20°–80°, with a step size of 0.02°. The obtained diffraction patterns were compared with standard JCPDS data to confirm the formation of the delafossite phase and to evaluate the influence of Fe doping on the lattice parameters. FTIR analysis was performed using a PerkinElmer spectrometer in the wavenumber range of 4000–400 cm^{-1}. This analysis provided insights into the chemical bonding, functional groups, and structural integrity of the synthesized nanoparticles. Peaks corresponding to metal-oxygen bonds confirmed the successful incorporation of Fe into the $CuAlO_2$ matrix. The optical absorption spectra of the synthesized samples were recorded using a Lambda-950 UV-Vis-NIR spectrophotometer. Sunlight was employed as a photon source for photocatalytic activity measurements. The optical band gap of the materials was estimated using Tauc's plot method from the absorption data, which helped evaluate the effect of Fe doping on the light absorption capabilities of $CuAlO_2$. The electrical properties, including frequency-dependent capacitance, loss parameters, and AC conductivity, were thoroughly examined using a Hioki 3532 LCR meter. Measurements were conducted at room temperature under varying frequencies to understand the impact of Fe doping on the electrical behavior of the nanoparticles.

The photocatalytic activity of the synthesized Fe-doped $CuAlO_2$ nanoparticles was assessed by evaluating their performance in degrading organic pollutants. The experiments utilized sunlight as the photon source, and the degradation rate of the pollutants was monitored using UV-Vis spectrophotometry. The enhancement in photocatalytic efficiency due to Fe doping was analyzed by comparing the degradation rates of the doped and undoped samples.

3. RESULTS AND DISCUSSION

The X-ray diffraction (XRD) pattern of $Cu_{0.9}Fe_{0.1}AlO_2$ nanoparticles (Figure 1) reveals well-defined peaks corresponding to specific crystallographic planes, confirming the formation of the delafossite structure. The diffraction peaks observed at 2θ values near 32°, 36°, 39°, and 54° correspond to the (006), (101), (012), and (104) planes, respectively, which align with the standard reference patterns for $CuAlO_2$. The sharpness of the peaks indicates a highly crystalline nature of the synthesized nanoparticles. The absence of secondary peaks confirms the purity of the sample and the successful incorporation of Fe ions into the $CuAlO_2$ lattice without significant phase segregation.

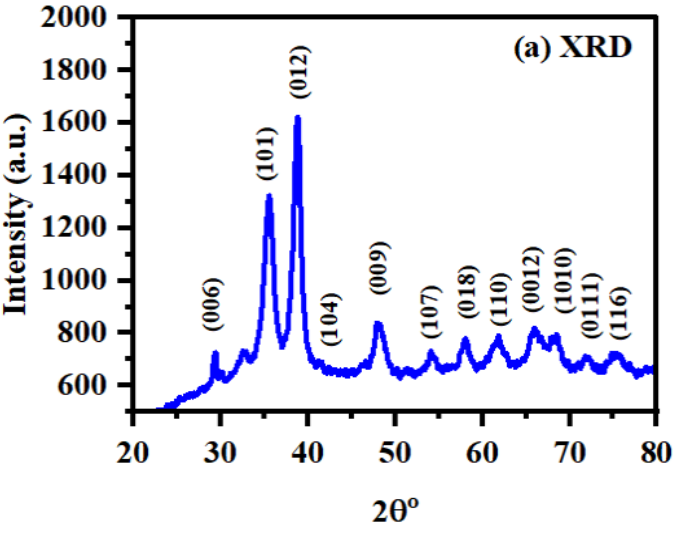

Fig. 1. XRD pattern of $Cu_{0.9}Fe_{0.1}AlO_2$ nanoparticle.

The slight shifts in peak positions and changes in intensities observed compared to pristine $CuAlO_2$ may be attributed to the substitution of Fe ions into the $CuAlO_2$ lattice. This substitution likely alters the unit cell parameters due to the slightly different ionic radii of Fe^{3+} (0.645 Å) and Cu^{1+} (0.74 Å). Such lattice distortions could modify the electron density distribution and potentially affect the material's electronic and optical properties. These structural changes further validate the successful doping of Fe into $CuAlO_2$ and provide insight into the material's suitability for advanced applications, such as photocatalysis and electronic devices.

The Fourier Transform Infrared (FTIR) spectrum of $Cu_{0.9}Fe_{0.1}AlO_2$ (Figure 2) displays characteristic absorption bands that confirm the formation of the desired structure. The broad band observed around 2880 cm^{-1} is attributed to C-H stretching vibrations, which could stem from residual organic species from the sol-gel synthesis process. The band at 1385 cm^{-1} corresponds to C-H bending vibrations. Most notably, the sharp peak near 500 cm^{-1} is assigned to Cu-O and Al-O stretching vibrations, confirming the presence of metal-oxide bonds that form the backbone of the delafossite structure. The absence of significant peaks related to other impurities or undesired functional groups further corroborates the high purity of the synthesized material. The pronounced metal-oxide peak suggests a robust delafossite lattice, which is critical for ensuring stability and functional properties in practical applications.

The UV-visible absorption spectrum of $Cu_{0.9}Fe_{0.1}AlO_2$ (Figure 3(a)) exhibits strong absorption in the ultraviolet

region, with an absorption edge at approximately 400 nm. This suggests that the material is capable of absorbing UV light efficiently, making it a potential candidate for photocatalytic applications. The band gap energy, determined using the Tauc plot (Figure 3(b)), is approximately 2.8 eV. This value aligns with the material's suitability for visible-light-driven photocatalysis. The incorporation of Fe into the $CuAlO_2$ matrix likely introduces localized states within the band gap, which could enhance light absorption and improve charge carrier separation. These characteristics are essential for maximizing the photocatalytic degradation of pollutants and harnessing solar energy. Furthermore, the band gap value indicates the material's potential for applications in photoelectrochemical cells and optoelectronic devices.

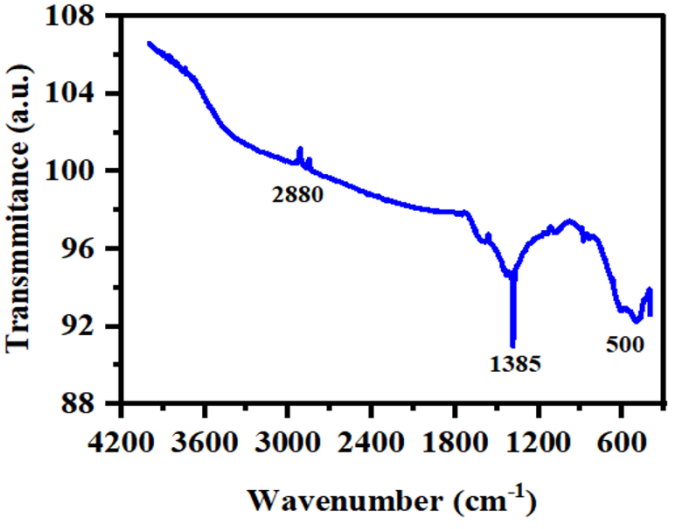

Fig. 2. FTIR spectrum of $Cu_{0.9}Fe_{0.1}AlO_2$ nanoparticle.

The dielectric properties of $Cu_{0.9}Fe_{0.1}AlO_2$ were investigated across a range of frequencies (Figure 4). The real part of the dielectric constant (ε′) exhibits a frequency-dependent behavior, decreasing with increasing frequency (Figure 4(a)). This dispersion is attributed to the inability of dipoles to follow the alternating electric field at higher frequencies. At lower frequencies, the higher ε′ values suggest the dominance of interfacial polarization mechanisms, which are common in heterogeneous materials. The imaginary part of the dielectric constant (ε″) also decreases with frequency, indicating reduced dielectric losses at higher frequencies (Figure 4(b)). This behavior is advantageous for high-frequency electronic applications, where energy dissipation must be minimized. The dielectric loss tangent (tan δ) (Figure 4(c)) follows a similar trend, with decreasing values at higher frequencies. This indicates that $Cu_{0.9}Fe_{0.1}AlO_2$ exhibits minimal energy dissipation, making it a promising candidate for applications in capacitors and other high-frequency electronic devices. The AC conductivity (σ) (Figure 4(d)) increases with frequency, which is indicative of a hopping conduction mechanism. This suggests that charge carriers move via localized states, which are likely introduced by Fe doping. While the overall conductivity values are relatively low, this could be attributed to the presence of defects or impurities that impede charge carrier mobility. Future work could focus on optimizing the synthesis process to enhance the conductivity and broaden the material's applicability.

The photocatalytic performance of $Cu_{0.9}Fe_{0.1}AlO_2$ was evaluated using methylene blue (MB) dye degradation under sunlight irradiation (Figure 5). The material exhibited a degradation efficiency of approximately 34% after 140 minutes, with a rate constant (k) of 0.00302 min^{-1}. While these values indicate moderate photocatalytic activity, several factors may limit the performance:

Dopant Concentration: The Fe dopant concentration may be insufficient to generate the optimal number of active sites for photocatalytic reactions.

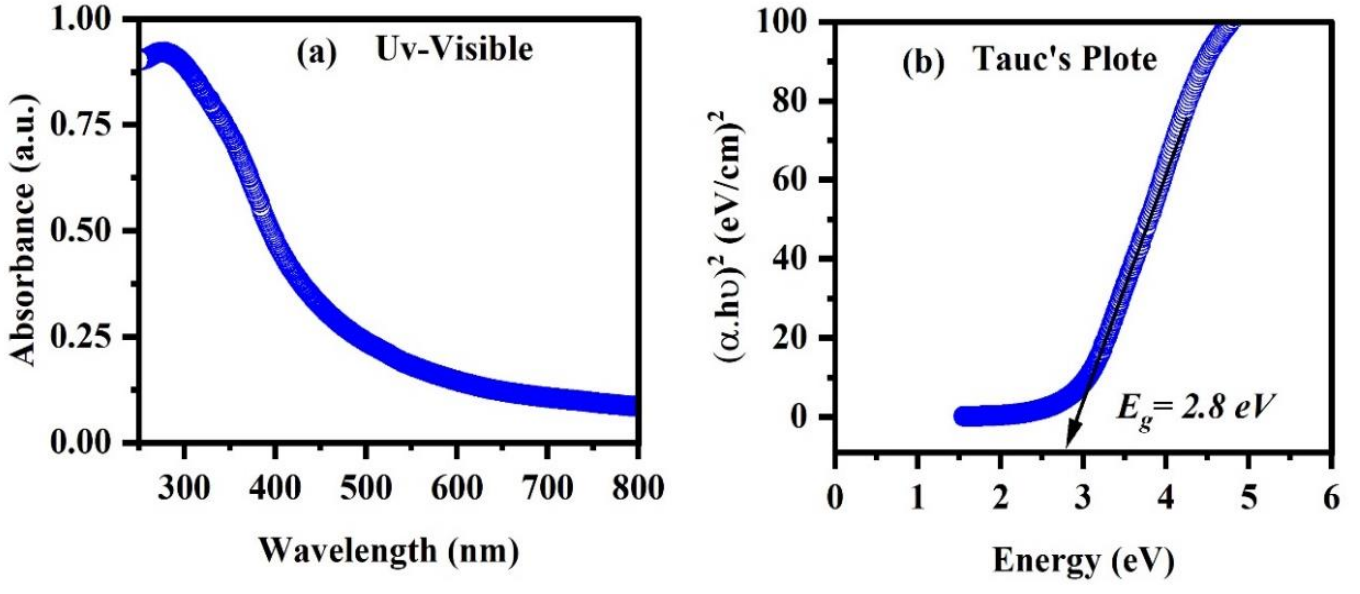

Fig. 3. (a) UV-visible absorbance (b) Tauck's Plote spectra of $Cu_{0.9}Fe_{0.1}AlO_2$ heterostructure nanoparticles.

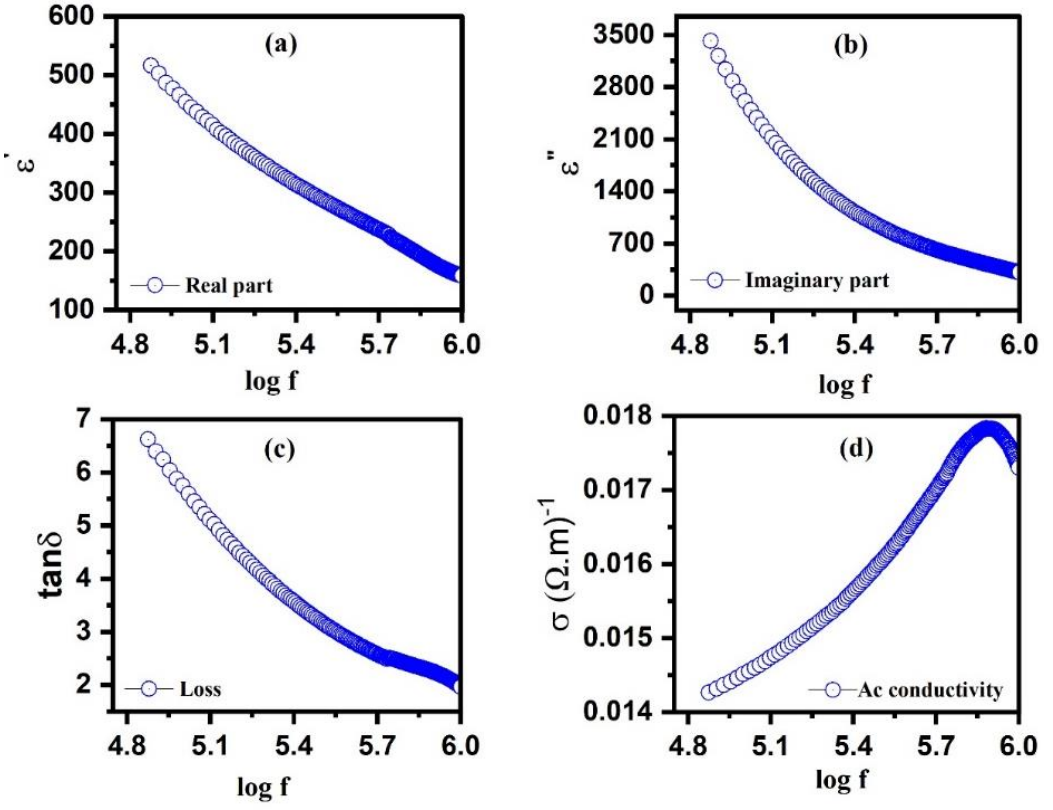

Fig. 4. Room temperature: (a) real part, (b) imaginary part of dielectric constant, (c) Loss, and (d) ac conductivity of $Cu_{0.9}Fe_{0.1}AlO_2$.

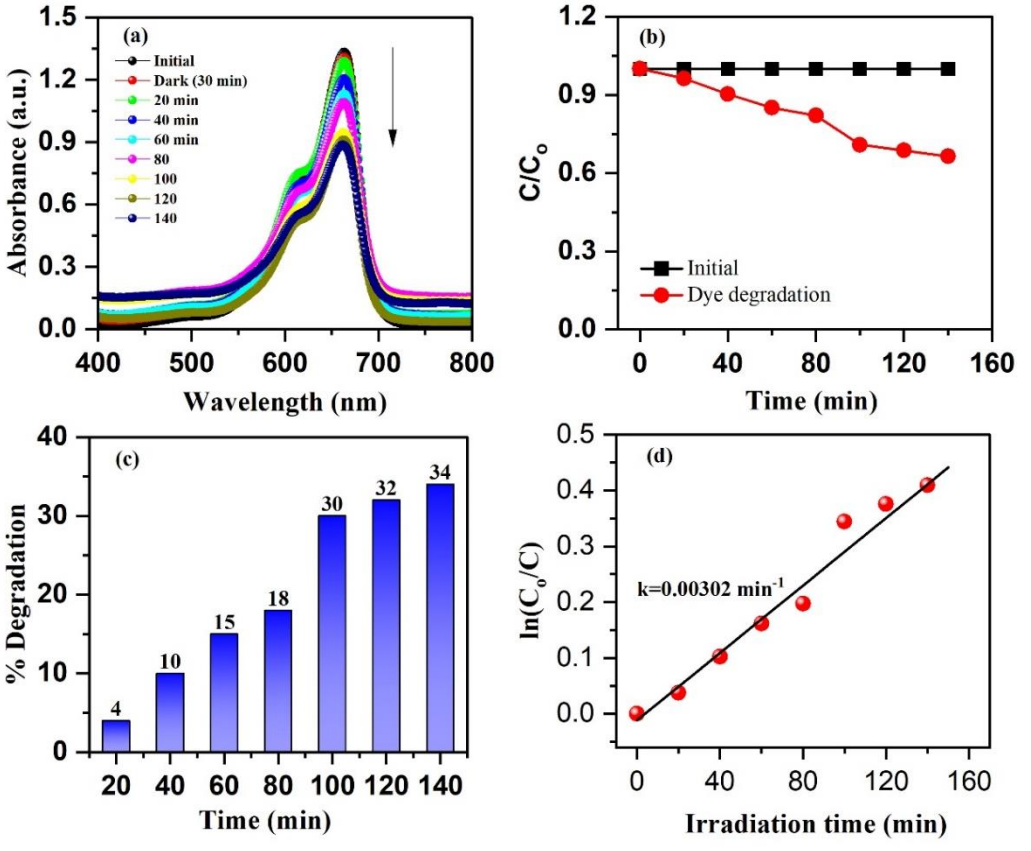

Fig. 5. Photocatalytic Activity of $Cu_{0.9}Fe_{0.1}AlO_2$ Nanoparticles (a) Photodegradation of MB dye (b) Variation of C/C*o* of control MB dye (c) Bar chart showing the percentage of MB degradation over time (d) Determination of the rate constant (k) for the photocatalytic degradation process.

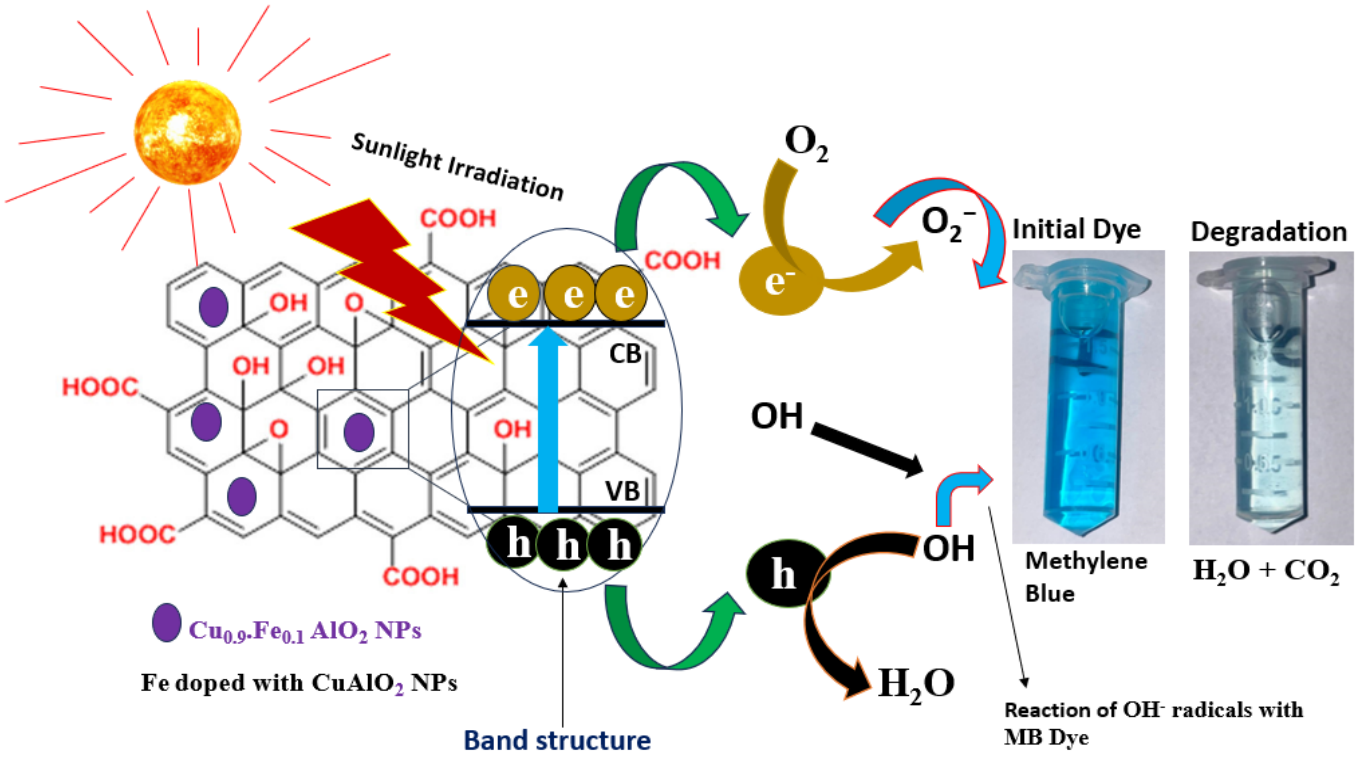

Fig. 5. Schematic Overview of the Photocatalytic Mechanism with $Cu_{0.9}Fe_{0.1}AlO_2$ nanostructures.

Charge Carrier Dynamics: The high recombination rate of electron-hole pairs could reduce the availability of reactive species required for dye degradation.

Surface Area and Morphology: A suboptimal surface area and particle morphology could limit the accessibility of active sites and impede charge transfer.

Light Absorption: Although the material absorbs UV light effectively, its absorption in the visible region could be improved to enhance photocatalytic performance.

To address these challenges, future studies could explore higher dopant concentrations, co-doping strategies, or surface modifications to improve light absorption and charge carrier dynamics. Additionally, optimizing synthesis parameters to achieve a higher surface area and better particle morphology could further enhance the material's photocatalytic efficiency.

The proposed mechanism for MB dye degradation (Figure 6) involves the generation of electron-hole pairs upon light irradiation. The photogenerated electrons react with oxygen molecules to form reactive oxygen species (ROS), such as superoxide radicals ($O_2^{-}\cdot$), while the holes oxidize water molecules to generate hydroxyl radicals (·OH). These reactive species collectively degrade the dye molecules into smaller, less harmful compounds.

The combined structural, optical, and dielectric properties of $Cu_{0.9}Fe_{0.1}AlO_2$ nanoparticles highlight their versatility for multiple applications. The high crystallinity and stable delafossite structure make them suitable for electronic devices, while their moderate photocatalytic activity suggests potential for environmental remediation. The material's dielectric properties, particularly its low dielectric loss and stable conductivity, position it as a promising candidate for high-frequency capacitors and sensors. However, further optimization is necessary to fully realize the material's potential. Enhancing the photocatalytic performance through advanced doping strategies or surface engineering could broaden its applicability in water treatment and solar energy conversion. Similarly, improving charge carrier mobility could expand its use in electronic and optoelectronic devices. Fe-doped $CuAlO_2$ nanoparticles exhibit a unique combination of properties that make them suitable for diverse applications. Continued research and development in synthesis optimization and property enhancement will pave the way for their integration into advanced technologies.

4. CONCLUSION

This study explored the synthesis, characterization, and multifunctional properties of Fe-doped $CuAlO_2$ nanoparticles for energy harvesting applications. The successful substitution of iron at the copper site in the delafossite $CuAlO_2$ structure was confirmed through XRD, FTIR, and UV-visible spectroscopy, which validated the material's crystalline integrity, chemical bonding, and optical band gap. Electrical conductivity measurements revealed a significant enhancement upon iron doping, driven by the introduction of additional charge carriers and improved dielectric properties.

These findings underscore the potential of Fe-doped $CuAlO_2$ for use in electronic devices and energy storage systems, where high conductivity and low dielectric loss are essential. The photocatalytic activity of the synthesized nanoparticles, as demonstrated by the degradation of methylene blue dye under visible light irradiation, further emphasizes their utility in environmental remediation. Although the observed photocatalytic efficiency was moderate (34% degradation in 140 minutes), it provides a solid foundation for further research. The moderate performance is attributed to factors such as dopant concentration, charge recombination rates, and surface morphology, highlighting the need for optimization in these areas. The dual benefits of enhanced electrical conductivity and visible light-driven photocatalytic activity position Fe-doped $CuAlO_2$ nanoparticles as versatile materials for sustainable energy applications. Their potential spans solar energy harvesting, photocatalysis, and advanced optoelectronic devices. Future research should focus on optimizing the synthesis process, exploring co-doping strategies, and refining experimental conditions to maximize performance. These efforts could pave the way for the practical deployment of Fe-doped $CuAlO_2$ in renewable energy and environmental technologies, contributing to global sustainability goals.

DECLARATIONS

Ethical Approval

Not Applicable

Funding

Not applicable

Availability of data and material

The data of the manuscript are available upon request.

Conflicts of Interest

The authors declare no conflicts of interests. The authors alone are responsible for the content and writing of this article.

Authors' contributions

All the authors contribute equally to the article, in writing and editing

ACKNOWLEDGEMENTS

Authors are thankful to the Council of Science and Technology (CST) U.P. India for providing financial assistance under Project No. CST/D-1519.

REFERENCES

[1] Abdelhamid, H.N., **2015**, December. Delafossite nanoparticle as new functional materials: advances in energy, nanomedicine and environmental applications. In *Materials Science Forum* (Vol. 832, pp. 28-53). Trans Tech Publications Ltd.

[2] Marquardt, M.A., Ashmore, N.A. and Cann, D.P., **2006.** Crystal chemistry and electrical properties of the delafossite structure. *Thin Solid Films*, *496*(1), pp.146-156.

[3] Afonso, C., Lima Jr, O., Segundo, I.R., Landi Jr, S., Margalho, É., Homem, N., Pereira, M., Costa, M.F., Freitas, E. and Carneiro, J., **2022.** Effect of iron-doping on the structure and photocatalytic activity of TiO_2 nanoparticles. *Catalysts*, *13*(1), p.58.

[4] Chakhari, W., Naceur, J.B., Taieb, S.B., Assaker, I.B. and Chtourou, R., **2017.** Fe-doped TiO_2 nanorods with enhanced electrochemical properties as efficient photoanode materials. *Journal of Alloys and Compounds*, *708*, pp.862-870.

[5] Khan, M.M., Siwach, R., Kumar, S. and Alhazaa, A.N., **2019**. Role of Fe doping in tuning photocatalytic and photoelectrochemical properties of TiO_2 for photodegradation of methylene blue. *Optics & Laser Technology*, *118*, pp.170-178.

[6] Agrawal, S., Parveen, A. and Azam, A., **2016.** Influence of Mg on structural, electrical and magnetic properties of $CuAlO_2$ nanoparticles. *Materials Letters*, *168*, pp.125-128.

[7] Sarabia, M.A., Rojas, S.D., López-Cabaña, Z., Villalba, R., González, G. and Cabrera, A.L., **2016**. Carbon dioxide adsorption studies on delafossite $CuFeO_2$ hydrothermally synthesized. *Journal of Physics and Chemistry of Solids*, *98*, pp.271-279.

[8] Prakash, T., Ramasamy, S. and Murty, B.S., **2013**. Effect of DC bias on dielectric properties of nanocrystalline $CuAlO_2$. *Electronic Materials Letters*, *9*, pp.207-211.

[9] Zhao, Q.M., Zhao, Z.Y., Liu, Q.L., Yao, G.Y. and Dong, X.D., **2020.** Delafossite $CuGaO_2$ as promising visible-light-driven photocatalyst: synthesize, properties, and performances. *Journal of Physics D: Applied Physics*, *53*(13), p.135102.

[10] Zhang, J.X., Zhao, Z.Y., Yang, T.L., Yang, J., Zhang, J., Liu, Q.J. and Kuang, Y., **2024.** Harnessing intrinsic defect complexes for visible-light-driven photocatalytic activity in Delafossite $CuAlO_2$. *Acta Materialia*, *269*, p.119801.

[11] Wang, C., Zhu, H., Meng, Y., Nie, S., Zhao, Y., Shin, B., Fortunato, E., Martins, R., Shan, F. and Liu, G., **2019.**

Sol–gel processed p-type $CuAlO_2$ semiconductor thin films and the integration in transistors. *IEEE Transactions on Electron Devices*, *66*(3), pp.1458-1463.

[12] Chiu, S.H. and Huang, J.C.A., **2013.** Characterization of p-type $CuAlO_2$ thin films grown by chemical solution deposition. *Surface and Coatings Technology*, *231*, pp.239-242.

[13] Yu, R.S. and Yin, H.H., **2012.** Structural and optoelectronic properties of p-type semiconductor $CuAlO_2$ thin films. *Thin Solid Films*, *526*, pp.103-108.

[14] Amrute, A.P., Łodziana, Z., Mondelli, C., Krumeich, F. and Pérez-Ramírez, J., **2013.** Solid-state chemistry of cuprous delafossites: Synthesis and stability aspects. *Chemistry of Materials*, *25*(21), pp.4423-4435.

[15] Chang, Y.H., Wang, H., Siao, T.F., Lee, Y.H., Bai, S.Y., Liao, C.W., Zhuang, J.K., Chiu, T.W. and Kuo, C.H., **2021**. A new solution route for the synthesis of $CuFeO_2$ and Mg-doped $CuFeO_2$ as catalysts for dye degradation and CO_2 conversion. *Journal of Alloys and Compounds*, *854*, p.157235.

[16] Khan, A., Valicsek, Z., Horváth, O., Khan, M.M. and Wafi, A., **2024.** Ferrite-based photocatalysts: Synthesis, modifications, and key parameters in photocatalytic-related applications. *Materials Today Communications*, *40*, p.109556.

[17] Lalanne, M., Demont, P. and Barnabé, A., **2011.** Ac conductivity and dielectric properties of $CuFe_{1-x}Cr_xO_2$: Mg delafossite. *Journal of Physics D: Applied Physics*, *44*(18), p.185401.

[18] Traiphop, S., Thongbai, P. and Kamwanna, T., **2020.** Effect of synthesis method on magnetic and dielectric properties of $CuBO_2$ delafossite oxide. *Journal of the Australian Ceramic Society*, *56*(2), pp.499-505.

[19] Wang, C., Zhu, H., Meng, Y., Nie, S., Zhao, Y., Shin, B., Fortunato, E., Martins, R., Shan, F. and Liu, G., **2019.** Sol–gel processed p-type $CuAlO_2$ semiconductor thin films and the integration in transistors. *IEEE Transactions on Electron Devices*, *66*(3), pp.1458-1463.

[20] Yu, S.M. and Zhao, Z.Y., **2023.** Tailoring doping locations and types for high-performance $CuFeO_2$-based photocatalysts. *Journal of the American Ceramic Society*, *106*(12), pp.7582-7595.

[21] Liu, Q.L., Zhao, Z.Y., Zhao, R.D. and Yi, J.H., **2020.** Fundamental properties of delafossite $CuFeO_2$ as photocatalyst for solar energy conversion. *Journal of Alloys and Compounds*, *819*, p.153032.

[22] El-Bassuony, A.A. and Abdelsalam, H.K., **2018.** Attractive improvement in structural, magnetic, optical, and antimicrobial activity of silver delafossite by Fe/Cr doping. *Journal of Superconductivity and Novel Magnetism*, *31*(11), pp.3691-3703.

[23] Hossain, S.A., Sarkar, S., Bose, S. and Das, P., **2023**. Synthesis, characterization, and application of delafossites as catalysts for degrading organic pollutants and degradation mechanisms: A detailed insight. *Surfaces and Interfaces*, p.103281.

